

Machine Learning for the Gravitational Wave Observation with Pulsar Timing Array

Jin Li^{✉,1} MengNi Chen,¹ Yi Feng,^{2,3,4} Di Li,^{4,5} and Yuanhong Zhong⁶

¹*Department of Physics, Chongqing University, Chongqing 401331, China**

²*National Astronomical Observatories, Chinese Academy of Sciences, Beijing 100012, China*

³*University of Chinese Academy of Sciences, Beijing 100049, China*

⁴*CAS Key Laboratory of FAST, National Astronomical Observatories, Chinese Academy of Sciences, Beijing 100101, China*

⁵*NAOC-UKZN Computational Astrophysics Centre, University of KwaZulu-Natal, Durban 4000, South Africa*

⁶*College of Microelectronics and Communication Engineering, Chongqing University, Chongqing 401331, China*

(Dated: April 1, 2020)

Pulsar timing arrays (PTAs) have been proven as one of the most potential approaches to detect low-frequency gravitational waves in the near future. Although PTAs have not captured any GW signals at present, there have been a large number of related theoretical researches and some meaningful detection limits. In this paper, we focus on the nanohertz gravitational waves (GWs) from individual supermassive binary black holes (SMBBHs). Given a specific pulsar PSR J1909–3744, the corresponding GW–induced timing residuals in PTAs with Gaussian white noise can be simulated. Then we present the classification of simulated PTA data and parameter estimation for potential GW sources using machine learning based on neural networks. As a classifier, the convolutional neural network (CNN) shows a great performance when the signal to noise ratio ≥ 7 (the corresponding dimensionless amplitude of GW is $h \geq 2 \times 10^{-15}$). On the other hand, we apply recurrent neural network (RNN) and Bayesian neural networks (BNN) to chirp mass (\mathcal{M}) estimation, which are able to provide the mean relative error and uncertainties of \mathcal{M} . That is crucial to astrophysical observation. In our case, the mean relative error of chirp mass estimation is less than 15% with PTA sensitivity. Although these results are achieved for simulated PTA data, it's important for realizing intelligent processing on PTA data analysis.

Keywords: Machine Learning; Neural Network; PTA; GW-induced time residuals

PACS numbers: 04.30.Db; 07.05.Mh

I. INTRODUCTION

As a supplement to the direct detection of Gravitational Waves (GWs), using Pulsar Timing Arrays (PTAs) to detect nanohertz GWs is considered as another major milestone in GW astrophysics following the detection of Gravitational Waves (GWs) in LIGO frequency band. The target of GWs detection by PTAs is to recognize the influence of GW on the arrival time of pulsar signals at Earth. The continuous wave from individual inspiralling supermassive binary black holes (SMBBHs) is one of the promising GW sources in nanohertz frequency range [1]. And there has been significant improvement on such GW signal search in PTA data [2]. Therefore we focus on the GWs from individual SMBBHs to investigate the effectiveness of machine learning based on neural networks on PTA data analysis.

Although the statistically significant GW has not been detected yet, the upper limits on the detectable GW strain amplitude in PTA frequency range are constantly improved (such as $h \geq 1.7 \times 10^{-14}$ at 10^{-8} Hz now). At the same time, the sensitive values of GW source (i.e., SMBBHs) parameters are derived, which are chirp mass $\mathcal{M} \sim 10^9 M_\odot$, luminosity distance $D_L \sim 100$ Mpc [1]. These results are derived by matched filtering method [3], since the signal model is clear. In this paper, we adopt a completely different data analysis method—machine learning based on neural networks to identify GW signal and estimate the chirp mass of SMBBHs.

With the development of intelligent data processing technologies, machine learning based on neural network exhibits great potential to realize real-time GW searches. Many researches about classification and regression of GWs in LIGO/Virgo frequency band by means of deep learning algorithms have been presented in [4–7]. These works show applying deep learning to search GWs from binary black hole mergers is capable to achieve similar performance while several orders of magnitude faster than matched-filtering, and significantly surpasses traditional machine learning techniques. Furthermore the most outstanding advantage is that deep learning can be extended to search some

*Electronic address: cqjinli1983@cqu.edu.cn

other kinds of gravitational wave signals not only GWs from binary black hole mergers [4, 5, 8]. Meanwhile the parameters estimation using machine learning methods in other astronomical observations has also achieved a rapid development, such as applying convolutional Neural Networks (CNN) to automated analysis and uncertainties in parameters estimation of strong gravitational lenses [9, 10], using Recurrent Neural Network-Bayesian Neural Networks (RNN-BNN) to modifying dark energy models at higher redshift [11]. Inspired by these works, we adopt neural networks with different architectures to search simulated GWs signal in PTA data and estimate chirp mass of the GW source. The results we presented in this paper indicate that convolutional neural network is effective for GWs and noise classification in PTA time series. With such data processing it is expected to detect the GW with $h \geq 2 \times 10^{-15}$ from SMBBHs with $D_L \sim 75\text{Mpc}$. Meanwhile through training the networks with prior information, the feedforward networks (e.g. Elman neural network) are more suitable for parameters estimation and Bayesian neural networks (BNN) can acquire the uncertainty of chirp mass estimation after finding the optimal weights distribution. Those make our results more reliable and increase the confidence regions.

This paper is organized as follows: in section II, we describe the detailed process of simulating PTA timing residuals; Section III provides the structure of the deep learning network as classifier, and corresponding results; In section IV, the performance of Elman Neural Network and BNN adopted into parameter estimation are discussed. In the last section, some meaningful results and prospect are concluded.

II. OBTAINING THE SIMULATED DATA

The influence of GW on pulse arrival times (TOAs) can be derived from the GW-induced redshift of a pulse, which is given as

$$z(t, \Omega) = \frac{1}{2} \frac{\hat{u}^a \hat{u}^b}{1 + \hat{\Omega} \cdot \hat{u}} \Delta h_{ab}(t, \Omega), \quad (1)$$

where $\hat{\Omega}$ is a unit vector defining the direction of GW propagation, $\Delta h_{ab} = h_{ab}(t, \hat{\Omega}) - h_{ab}(t_p, \hat{\Omega})$ is the difference in the metric perturbation between the Earth and the pulsar, t and t_p are the times when the GW is passing the solar system barycenter and the pulsar respectively. Those have the relationship as $t_p = t - d_p(1 + \hat{\Omega} \cdot \hat{u})$, d_p is the distance to the pulsar, \hat{u} is the unit propagation vector of a pulse signal from the pulsar. Then an offset pulsar TOA (i.e. timing residuals) can be calculated through integrating the GW-induced redshift over the whole observing time as

$$s(t) = \int_0^t z(t') dt'. \quad (2)$$

Due to an individual GW source, the corresponding timing residuals can be derived as

$$s(t, \hat{\Omega}) = (F^+(\hat{\Omega}) \cos 2\psi + F^\times(\hat{\Omega}) \sin 2\psi) \Delta s_+(t) + (F^+(\hat{\Omega}) \sin 2\psi - F^\times(\hat{\Omega}) \cos 2\psi) \Delta s_\times(t), \quad (3)$$

where ψ is the polarization angle of GW, $F^+(\hat{\Omega})$ and $F^\times(\hat{\Omega})$ are antenna pattern response functions encoding the response of a given pulsar to a particular GW source, which are [12]

$$\begin{aligned} F^+ &= \frac{1}{4(1 - \cos \theta)} \{ (1 + \sin^2 \delta) \cos^2 \delta_p \cos [2(\alpha - \alpha_p)] \\ &\quad - \sin 2\delta \sin 2\delta_p \cos(\alpha - \alpha_p) + \cos^2 \delta (2 - 3 \cos^2 \delta_p) \}, \\ F^\times &= \frac{1}{2(1 - \cos \theta)} \{ \cos \delta \sin 2\delta_p \sin(\alpha - \alpha_p) \\ &\quad - \sin \delta \cos^2 \delta_p \sin [2(\alpha - \alpha_p)] \}, \end{aligned} \quad (4)$$

where $\cos \theta = \cos \delta \cos \delta_p \cos(\alpha - \alpha_p) + \sin \delta \sin \delta_p$. On the other hand, the GW-induced timing residuals should be considered as the comprehensive effect of Earth and the pulsar's conditions, which can be described as

$$\begin{aligned} \Delta s_{+, \times}(t) &= s_{+, \times}(t) - s_{+, \times}(t_p), \\ t_p &= t - d_p(1 - \cos \theta)/c, \end{aligned} \quad (5)$$

where $s_{+,\times}(t)$ is the Earth term and $s_{+,\times}(t_p)$ is the pulsar term. According to the Peter-Mathews GW waveforms[13], the pulsar timing residuals induced by an eccentric SMBBHs[14] are given as:

$$\begin{aligned} s_+(t) &= \sum_n - (1 + \cos^2 \iota) [a_n \cos(2\gamma) - b_n \sin(2\gamma)] \\ &\quad + (1 - \cos^2 \iota) c_n, \\ s_\times(t) &= \sum_n 2 \cos \iota [b_n \cos(2\gamma) + a_n \sin(2\gamma)], \end{aligned} \quad (6)$$

where

$$\begin{aligned} a_n &= -\zeta \omega^{-1/3} [J_{n-2}(ne) - 2eJ_{n-1}(ne) + (2/n)J_n(ne) \\ &\quad + 2eJ_{n+1}(ne) - J_{n+2}(ne)] \sin[nl(t)], \\ b_n &= \zeta \omega^{-1/3} \sqrt{1-e^2} [J_{n-2}(ne) - 2J_n(ne) \\ &\quad + J_{n+2}(ne)] \cos[nl(t)], \\ c_n &= (2/n)\zeta \omega^{-1/3} J_n(ne) \sin[nl(t)]. \end{aligned} \quad (7)$$

Here m_1 and m_2 are the component masses of binary black holes, which define the chirp mass $\mathcal{M}^{5/3} = m_1 m_2 (m_1 + m_2)^{-1/3}$, $\zeta = (G\mathcal{M})^{5/3}/c^4 D_L$, D_L is the luminosity distance of binary black holes, while e is the eccentricity. $\omega = 2\pi f$, f is the orbital frequency, $l(t)$ is the mean anomaly and γ is the initial angle of periastron, ι is the inclination angle of the orbit of binary black holes.

In this paper, we choose PSR J1909–3744 as the specific pulsar, which has been proven as one of the best high-time-precision pulsars[2]. According to above equations, the simulated GW-induced timing residuals with stationary Gaussian white noise can be obtained. All the parameters for simulation are listed in Table I.

TABLE I: The pulsar and GW source parameters for our simulation. Here Ra, Dec are right ascension and declination of object location at a celestial sphere frame coordinate. Due to the existence of measurement error, the pulsar distance is not a fixed value.

Pulsar (PSR J1909–3744)	Ra _p = 287.44764447874996 rad Dec _p = –37.73735187222222 rad
GW source	Ra _g = 214.49791667 rad Dec _g = 25.13666667 rad
Luminosity distance of binary black holes (Mpc)	75
Orbital frequency of binary black holes (Hz)	$2.15 \times 10^{-9} \sim 2.43 \times 10^{-9}$
Eccentricity	0
Chirp mass (M_\odot)	$10^8 \sim 10^9$
Orbital inclination of binary black holes (rad)	$0.36 \sim 0.48$
Polarization of Gravitational Wave	$0 \sim \pi$
Initial pericentric angle (rad)	$3.23 \sim 3.84$
Initial phase	$0.72 \sim 0.83$
Pulsar distance (kpc)	$1.23 \sim 1.29$
Sampling frequency: approximately uniform sampling, sampling 393 times in 12 years	
Noise: Gauss white noise, which is 100 nanoseconds	

Assuming the noise in each sample is additive, the data for each set of pulsar timing residuals can be written as

$$d_i = s_i + n_i, \quad (8)$$

where $s_i = s(t_i, \boldsymbol{\lambda})$ is the GW-induced timing residuals in Eq.(3) and $\boldsymbol{\lambda}$ is the source parameters, $n_i = n(t_i)$ is the noise. In this work, we generate 20,000 data sets with different source and pulsar parameters, then randomly divide them into 10,000 training sets and 10,000 testing sets. Each set is similar to that shown in Fig.1(a). In order to investigate the ability of our neural network varying with the strength of GW, the training and testing sets are sorted

into several subsets with different signal to noise ratio (SNR). In the lower SNR intervals, we make more samples shown in Fig.1(b), that because machine learning needs more samples to learn the signal features with lower SNR. For each subset, the corresponding SNR is given as

$$\text{SNR} = \sqrt{(s_i | s_i)}, \quad (9)$$

where $(s_i | s_i) = \sum_i s_i \cdot s_i / \sigma^2$, σ^2 is the mean square of the residuals from the pulsar, which is also equal to the power of noise. In our case, $\sigma = 100\text{ns}$, and sampling frequency is 393 times in 12 years. At the same time, we ensure the training sets and testing sets without overlap, just as shown in Fig 2.

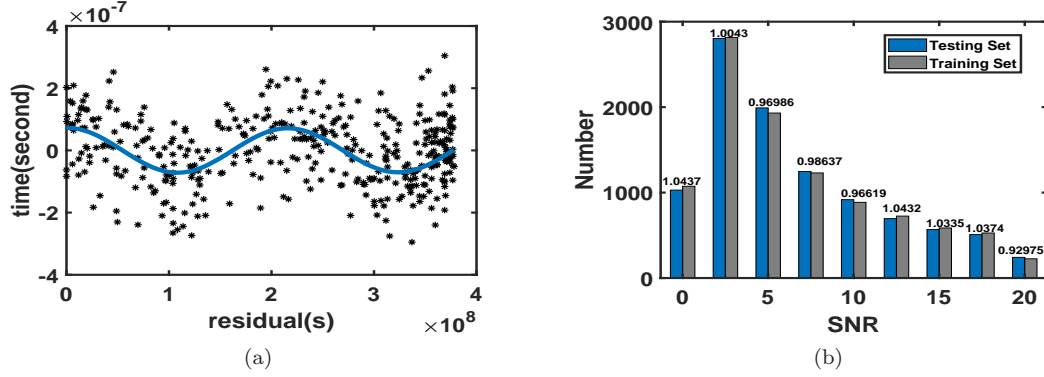


FIG. 1: (a) The simulated time-domain data of PTA as one sample in our training sets, which is in 1×393 dimension. Black points represent our simulated time residuals, and the blue solid line is the GW-induced time residuals (nanoseconds). (b) Distribution of training and testing samples in SNR intervals. On the column we mark the ratio of the number of testing sets to the number of training sets. The samples with lower SNR are chosen to be more than those with higher SNR, because we hope our neural network is capable to extract more signal features in lower SNR cases.

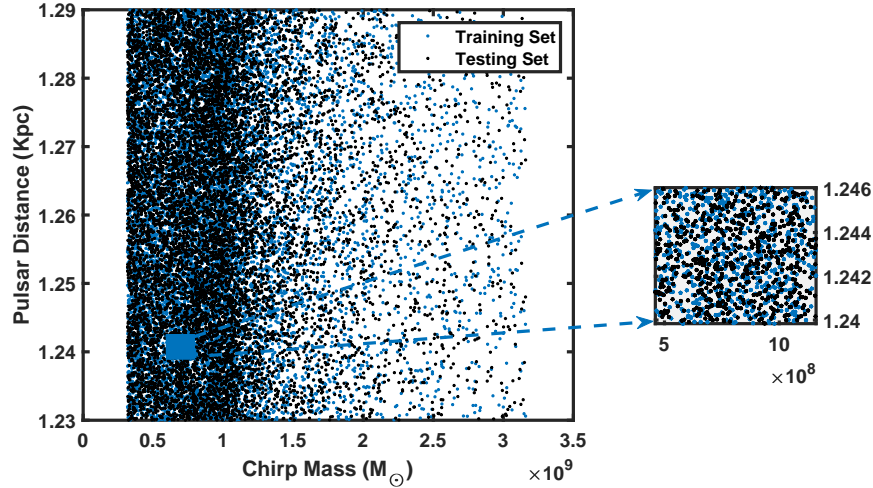


FIG. 2: Distribution of simulated data sets in chirp mass bank. The blue points represent the training sets, and the black points represent the testing sets. In the zoom plot, the distribution of chirp mass intervals is magnified from 0.5×10^9 to $1.0 \times 10^9 M_\odot$. Testing sets and training sets are distributed in the same way, but they are not overlapped.

III. MACHINE LEARNING FOR IDENTIFYING TOA VARIATIONS FROM INDIVIDUAL INSPIRALLING SUPERMASSIVE BINARY BLACK HOLES

The neural network model we used here is composed of convolutional layers and fully connected neural networks, which is motivated by several related works [4, 5, 8, 15–17]. Through adjusting hyperparameters manually, the optimal

values of them are listed in the caption of Table II. The training process begins with samples in larger SNR intervals, then switches to the ones in lower SNR intervals gradually. That can make the network to extract hidden information more easily and accurately [7].

TABLE II: The structure of the neural network used as a classifier. The number of neurons in the convolutional layers are 16, 8, 16 respectively. The kernel sizes are 1×2 for all the convolutional layers and 1×1 for all the pooling layers. The stride is set to be 1 for all of the convolutional layers and pooling layers. The dilation factor of the convolutional layers is set to be 1, and the padding size of the pooling layer is zero. The function of pooling is max. The active function is Relu.

Input	Matrix(1×393)
1 ReshapeLayer	3-tensor(size: $1 \times 1 \times 393$)
2 ConvolutionLayer	3-tensor(size: $16 \times 1 \times 2$)
3 PoolingLayer	3-tensor(size: $16 \times 1 \times 1$)
4 Ramp	3-tensor(size: $16 \times 1 \times 1$)
5 ConvolutionLayer	3-tensor(size: $8 \times 1 \times 2$)
6 PoolingLayer	3-tensor(size: $8 \times 1 \times 1$)
7 Ramp	3-tensor(size: $8 \times 1 \times 1$)
8 ConvolutionLayer	3-tensor(size: $16 \times 1 \times 2$)
9 PoolingLayer	3-tensor(size: $16 \times 1 \times 1$)
10 Ramp	3-tensor(size: $16 \times 1 \times 1$)
11 FlattenLayer	vector(size: 393)
12 DotPlusLayer	vector(size: 20)
13 Ramp	vector(size: 20)
14 DotPlusLayer	vector(size: 2)
15 SoftmaxLayer	vector(size: 2)
Output	class

In this process, our network is initialized by “Xavier” method. The algorithm is chosen to be ADAM, which is an optimization algorithm based on the traditional stochastic gradient descent algorithm. It can iteratively update the weights of neural networks according to the training data. Furthermore, the learning rate can be adjusted automatically based on the first moment mean[18].

As a supervised binary classification, the datasets including GW signal are labeled as Ture, otherwise labeled as False. The last layer is chosen to be SoftmaxLayer, which represents the softmax cross entropy loss is used.

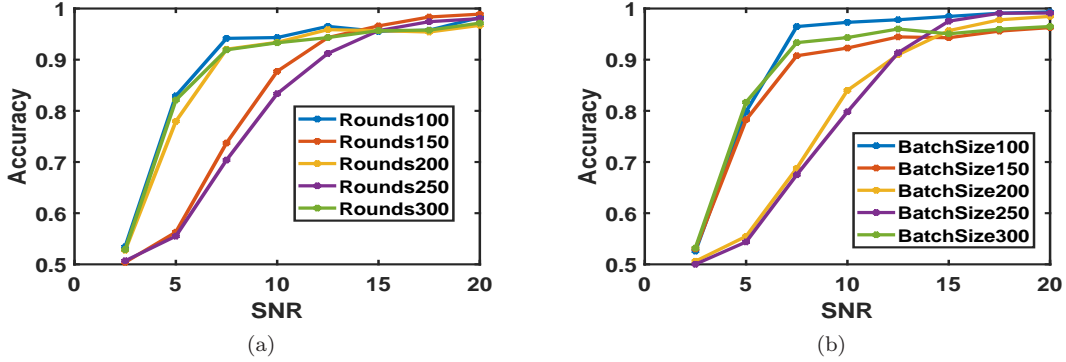


FIG. 3: (a) The accuracy varying with different MaxTrainingRounds ; (b) The accuracy varying with different Batchesizes.

Training the CNN network takes nearly 0.8 hours with NVIDIA GPU (Gtx1080ti, 11G ram). Its detection accuracy for identifying TOAs from GW with different SNRs is illustrated in Fig 3. The results show that the Maxtrainingrounds and Batch size both influence the identifying accuracy. On the whole, with SNR increasing the accuracy is enhanced, and the optimal Maxtrainingrounds and Batch size are both 100. In this case, our CNN detection accuracy can reach more than 95 percent when $\text{SNR} \geq 7$ (corresponding $h \geq 2 \times 10^{-15}$).

IV. MACHINE LEARNING BASED ON NEURAL NETWORKS FOR SOURCE PARAMETER ESTIMATION

Due to the degeneracy in luminosity distance and chirp mass of GW sources, we only concern the estimation of chirp mass \mathcal{M} given the luminosity distance D_L . Considering the time dependence on each data point, we find that Elman Neural Network has much better performance to estimate the source parameter than CNN, which is the earliest RNN, proposed by Elman in 1990. The recurrent neural network (RNN) has achieved a lot of success and wide application in many natural language processing. There are some similarities between the signal of GW and speech recognition (e.g. the data of the latter time is dependent on the previous data points). Therefore, the network's associative memory function is better and more stable. Elman neural network is a typical local regression network. It can be regarded as a recurrent neural network with local memory unit and local feedback connection. Its main structure is feedforward connection, including input layer, hidden layer and output layer. Its connection weight can be modified by learning. The transfer function of the hidden layer is a kind of non-linear function, generally a Sigmoid function, while that is linear function on output layer and the correlation layer.

TABLE III: The hyper-parameters of Elman Neural Network used for chirp mass estimation. The dimension of input is 1×393 , the training function is “traingdx” (Gradient descent method with momentum and adaptive learning rate)

Hyper Parameter	Value
Neuron Number	64
Learning Rate	0.0001
Maximum of iterations	10000
Error tolerance	10^{-5}
Maximum number of validation failures	6
Loss Function	Mean Squared Error (MSE)

Training the Elman neural network with different hyperparameters repeatedly, it took about thirteen minutes each time. The optimal values of some hyperparameters are listed in Table III. Using the Mean Relative Error to measure the performance of our neural network, the corresponding results are shown in Fig 4. With the increase of SNR, the mean relative error for chirp mass decreases properly, because the stronger GW signal in the data can be recognized more accurately. With current sensitivity of PTA, the mean relative error of chirp mass is $<15\%$.

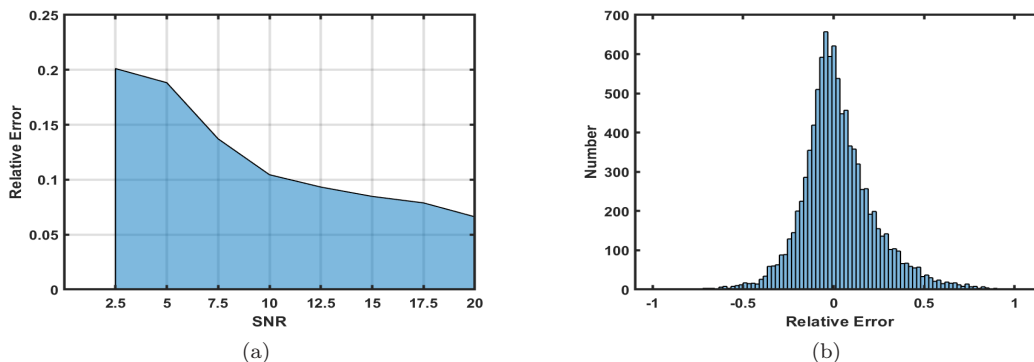


FIG. 4: (a) The mean relative error of chirp mass \mathcal{M} varies with SNR; (b) The histogram of the relative errors for all the testing samples

As an important issue of GW observation, the uncertainty of source parameter estimation can not be calculated by the network using point-estimation on weights (such as CNN and RNN). Therefore, we choose Bayesian neural network (BNN), which can predict the distribution of output using the prior distribution on network's weights and biases, to measure the uncertainty of estimation on objective source parameter.

Using Bayesian approach to estimate source parameter demands the neural networks to offer a probabilistic value of output. So the weights of these neural networks should have distributions instead of having deterministic values. In other words, our purpose is calculating the probabilistic distribution of each output value with a new testing input

by integrating over all possible weights, which can be expressed as

$$p(y^*|x^*, X, Y) = \int p(y^*|x^*, \omega) p(\omega|X, Y) d\omega, \quad (10)$$

where $X = x_1, \dots, x_N$ is the total samples of training input (x_i is a 1×393 time-series as Fig.1 (a)), and $Y = y_1, \dots, y_N$ is the corresponding labels. The posterior $p(\omega|X, Y)$ is usually approximated by a variational distribution $q(\omega)$. The optimizing process makes $q(\omega)$ as close as possible to the true distribution by minimizing their Kullback-Leibler (KL) distance, which measures the divergence between two distributions. Generally, we choose $q(\omega)$ to be a Gaussian distribution with σ_ω^2 variance and μ_ω mean value, which can be considered as the prior information. On the other hand, $p(y^*|x^*, \omega)$ means given the weights and input x^* the probability of outputting y^* , in practice which could be chosen as

$$p(y^*|x^*, \omega) = \frac{1}{\sqrt{2\pi}\sigma} \exp[(y^* - y)^T \sigma^{-1} (y^* - y)], \quad (11)$$

where σ is the prior standard deviation of y^* , which can be set as the prior standard deviation of weights (i.e., $\sigma = \sigma_\omega$). Then the neural networks need to find the optimal σ_ω and μ_ω through repeatedly training the networks with sampled weights from $q(\omega)$.

The hyper-parameters of our Bayesian Neural Network (BNN) are list in Table IV. In our case, X is a 12000×393 matrix, 12000 indicates the number of samples used to training. Y labels the corresponding chirp mass of X , which is 12000×1 accordingly. x^*, y^* represent a testing input and the corresponding expected chirp mass respectively. Fig.5 shows the estimated chirp mass against the true value of this parameter for 8000 testing samples. We can see that all the predicted values are within 1σ confidence level of a normal distribution. We also find our BNN is sensitive to the chirp mass in $6.5 \times 10^8 \sim 8.3 \times 10^8 M_\odot$, where the mean relative error is 18%.

TABLE IV: The hyper-parameters of Bayesian Neural Network (BNN) used for chirp mass estimation. The dimension of input is 1×393 . The network structure is a fully connected network, and the numbers of neurons in different layers are 64, 48, 128 and 24. Given the Gaussian Distribution as prior distribution, the mean square relative error is set as loss function.

Hyper Parameter	Value
Epoch	200
BatchSize	20
Learning Rate	10^{-6}
Prior Distribution	Gaussian Distribution
Active Function	Relu
Keep probability of dropout layer	0.97

V. CONCLUSION

We have investigated the effect of machine learning based on neural networks for PTA GW searches and corresponding source parameter estimation. According to the features of GW from individual SMBBHs, the simulated PTA time residuals are generated to train our neural networks. Through adjusting the hyperparameters of the neural networks, the CNN, RNN and BNN with optimal structure are obtained. Although this process takes several hours, the instant classification and parameter estimation with a specific SNR for testing samples can be achieved. From these results, we can determine the fundamental relation between the classification accuracy of the CNN and SNR of the data sets. Furthermore, we adopt a kind of RNN to do parameter estimation and obtain much better results than other machine learning methods, which indicates the RNN indeed can extract more information in time series data sets. By means of BNN, the errorbars of parameter prediction can be obtained, which provides important information for observation.

The main advantage of using machine learning to GW searches is that classification or prediction from a neural network is time-saving once the neural network has been trained well. Although our current work only refers to simulated data, it provides some feasible robust approaches for real PTA data analysis.

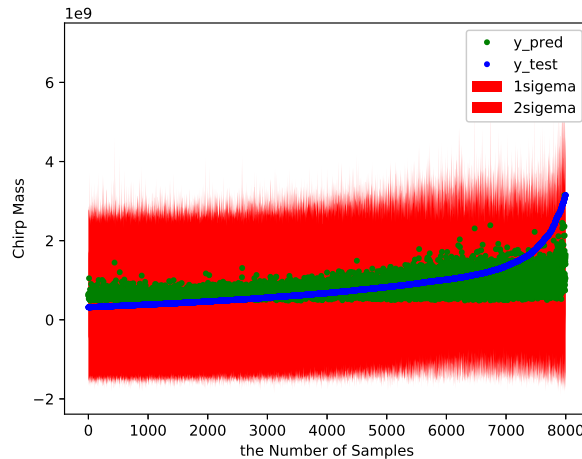


FIG. 5: The uncertainty of chirp mass estimation. The uncertainty contours in 1σ and 2σ are represented by red and light red respectively. The real values are blue dots and predicted values are green dots.

Acknowledgements

This work was supported by the National Natural Science Foundation of China (Grant Nos. 11873001, 11725313, 11690024), the Natural Science Foundation of Chongqing (Grant No. cstc2018jcyjAX0767), National Key R&D Program of China No. 2017YFA0402600, by the CAS International Partnership Program No.114A11KYSB20160008, by the CAS Strategic Priority Research Program No. XDB23000000.

-
- [1] Zhu X J, Hobbs G, Wen L, et al. An all-sky search for continuous gravitational waves in the Parkes Pulsar Timing Array data set. *Monthly Notices of the Royal Astronomical Society*, 2014, 444(4): 3709-3720.
 - [2] Feng Y, Li D, Li Y R, et al. Constraints on individual supermassive binary black holes using observations of PSR J1909-3744. *arXiv preprint arXiv:1907.03460*, 2019.
 - [3] Ellis J A, Jenet F A, McLaughlin M A. Practical methods for continuous gravitational wave detection using pulsar timing data. *The Astrophysical Journal*, 2012, 753(2): 96.
 - [4] George D, Huerta E A. Deep neural networks to enable real-time multimessenger astrophysics. *Physical Review D*, 2018, 97(4): 044039.
 - [5] George D, Huerta E A. Deep Learning for real-time gravitational wave detection and parameter estimation: Results with Advanced LIGO data. *Physics Letters B*, 2018, 778: 64-70.
 - [6] Allen G, Andreoni I, Bachelet E, et al. Deep Learning for Multi-Messenger Astrophysics: A Gateway for Discovery in the Big Data Era. *arXiv preprint arXiv:1902.00522*, 2019.
 - [7] Shen H, Huerta E A, Zhao Z. Deep Learning at Scale for Gravitational Wave Parameter Estimation of Binary Black Hole Mergers. *arXiv preprint arXiv:1903.01998*, 2019.
 - [8] George D, Shen H, Huerta E A. Glitch classification and clustering for LIGO with deep transfer learning. *arXiv preprint arXiv:1711.07468*, 2017.
 - [9] Levasseur L P, Hezaveh Y D, Wechsler R H. Uncertainties in Parameters Estimated with Neural Networks: Application to Strong Gravitational Lensing. *The Astrophysical Journal Letters*, 850:L7 (5pp), (2017)
 - [10] Hezaveh Y D, Levasseur L P, Marshall P J, Fast automated analysis of strong gravitational lenses with convolutional neural networks. *Nature* 548, p555-557 (2017)
 - [11] Celia E R, et al. A deep learning approach to cosmological dark energy models. *arXiv:1910.02788v1*
 - [12] Lee K J, et al. Gravitational wave astronomy of single sources with a pulsar timing array. *Monthly Notices of the Royal Astronomical Society* 414.4 (2011): 3251-3264.
 - [13] Peters P C, and Jon M. Gravitational radiation from point masses in a Keplerian orbit. *Physical Review* 131.1 (1963): 435.
 - [14] Taylor S R, et al. Detecting eccentric supermassive black hole binaries with pulsar timing arrays: resolvable source strategies. *The Astrophysical Journal* 817.1 (2016): 70.
 - [15] George D, Huerta E A. Deep neural networks to enable real-time multimessenger astrophysics[J]. *Physical Review D*, 2018, 97(4): 044039.

- [16] George D, Huerta E A. Deep Learning for real-time gravitational wave detection and parameter estimation: Results with Advanced LIGO data. *Physics Letters B*, 2018, 778: 64-70.
- [17] Fan X L, Li J, Li X, et al. Applying deep neural networks to the detection and space parameter estimation of compact binary coalescence with a network of gravitational wave detectors. *SCIENCE CHINA Physics, Mechanics Astronomy*, 2019, 62(6): 969512.
- [18] Kingma D P, Ba J Adam: A method for stochastic optimization. *arXiv preprint arXiv:1412.6980*, 2014.
- [19] Rebei A, Huerta E A, Wang S, et al. Fusing numerical relativity and deep learning to detect higher-order multipole waveforms from eccentric binary black hole mergers. *Physical Review D*, 2019, 100(4): 044025.
- [20] Nakano H, Narikawa T, Oohara K, et al. Comparison of various methods to extract ringdown frequency from gravitational wave data. *Physical Review D*, 2019, 99(12): 124032.
- [21] Razzano M, Cuoco E. Image-based deep learning for classification of noise transients in gravitational wave detectors. *Classical and Quantum Gravity*, 2018, 35(9): 095016.
- [22] Huerta E A, George D, Zhao Z, et al. Real-time regression analysis with deep convolutional neural networks[J]. *arXiv preprint arXiv:1805.02716*, 2018.
- [23] Vigeland S J, Islo K, Taylor S R, et al. Noise-marginalized optimal statistic: A robust hybrid frequentist-Bayesian statistic for the stochastic gravitational-wave background in pulsar timing arrays. *Physical Review D*, 2018, 98(4): 044003.
- [24] Ellis J A, Cornish N J. Transdimensional Bayesian approach to pulsar timing noise analysis. *Physical Review D*, 2016, 93(8): 084048.
- [25] Lee J, Bahri Y, Novak R, et al. Deep neural networks as gaussian processes. *arXiv preprint arXiv:1711.00165*, 2017.
- [26] Shen H, George D, Huerta E A, et al. Denoising gravitational waves using deep learning with recurrent denoising autoencoders. *arXiv preprint arXiv:1711.09919*, 2017.
- [27] Shen H, George D, Huerta E A, et al. Denoising Gravitational Waves with Enhanced Deep Recurrent Denoising Auto-Encoders, *ICASSP 2019-2019 IEEE International Conference on Acoustics, Speech and Signal Processing (ICASSP)*. IEEE, 2019: 3237-3241.
- [28] Vigeland S J, Islo K, Taylor S R, et al. Noise-marginalized optimal statistic: A robust hybrid frequentist-Bayesian statistic for the stochastic gravitational-wave background in pulsar timing arrays. *Physical Review D*, 2018, 98(4): 044003.
- [29] Wei W, Huerta E A. Gravitational Wave Denoising of Binary Black Hole Mergers with Deep Learning. *arXiv preprint arXiv:1901.00869*, 2019.
- [30] Verbiest J P W, Lentati L, Hobbs G, et al. The international pulsar timing array: first data release. *Monthly Notices of the Royal Astronomical Society*, 2016, 458(2): 1267-1288.
- [31] Taylor S R, Vallisneri M, Ellis J A, et al. Are we there yet? Time to detection of nanohertz gravitational waves based on pulsar-timing array limits. *The Astrophysical Journal Letters*, 2016, 819(1): L6.
- [32] Li X, Yu W, Fan X. A Method Of Detecting Gravitational Wave Based On Time-frequency Analysis And Convolutional Neural Networks. *arXiv preprint arXiv:1712.00356*, 2017.
- [33] Burke-Spolaor S, Taylor S R, Charisi M, et al. The astrophysics of nanohertz gravitational waves. *The Astronomy and Astrophysics Review*, 2019, 27(1): 5.
- [34] Gonzalez J A, Guzman F S. Characterizing the velocity of a wandering black hole and properties of the surrounding medium using convolutional neural networks. *Physical Review D*, 2018, 97(6): 063001.
- [35] Gabbard H, Williams M, Hayes F, et al. Matching matched filtering with deep networks for gravitational-wave astronomy. *Physical review letters*, 2018, 120(14): 141103.
- [36] Liu X J, Pulsar Timing Arrays and the Detection of Gravitational-wave Background. 2016.
- [37] Zhu X J, Detection of Gravitational Waves by Pulsar Timing Array, 2016(2):10-14.
- [38] Chua A J K, Galley C R, Vallisneri M. Reduced-order modeling with artificial neurons for gravitational-wave inference. *Physical Review Letters*, 2019, 122(21): 211101.